Identification of a vibration pattern from pressure measurements and radiation modes

Philippe Herzog, Régine Guillermin
LMA - CNRS, 31 chemin Joseph Aiguier, cedex 20, 13402 Marseille, France

Pierre Lorin
ABB Sécheron, Rue des Sablières 4-6, CH-1217 Meyrin, Switzerland

Vincent Chritin
IAV Engineering, Chemin des Couleuvres 4A, CH-1295 Tannay, Switzerland

Summary
The sound pressure radiated by a large transformer tank inside a power substation may be computed with a good accuracy from its vibration pattern, but this requires a high density of acceleration measurements, which are unconvenient and time-consuming. An alternative could be to use an holographic approach, using nearfield measurements to estimate the vibration pattern with a reasonable accuracy, or to compute the field propagated at larger distances with a better accuracy. This is however still difficult to perform on actual transformer tanks because the tank shape is often complex, and measurements very close to the tank raise security issues for an online transformer. The presented approach consists in using sparse pressure measurements performed at uneven locations (chosen to be compatible with practical constraints), and to estimate the vibration pattern as an expansion over a suitable set of functions defined over the tank boundary. Several studies suggest that the radiation modes of the tank are good candidates for this expansion, allowing a minimal number of terms for a targeted accuracy ; these modes are here numerically computed using a specific BEM code. A small inverse problem allows to estimate the expansion coefficents from sparse pressure measurements performed close enough to the vibrating surface. The radiated field may then be computed with good accuracy at locations further away. Simulations based on actual transformer vibration measurements allow to compare the pressure computed using a classical BEM approach, and its approximation using the above expansion.

PACS no. 43.40.Rj, 43.40.Sk, 43.60.Pt

1. Introduction

Many medium-sized distribution transformers must be located close enough to residential areas, where they cope with the growing demand of electric supply for modern cities. Although these devices are not very noisy, they may be considered as annoying by nearby inhabitants as they radiate a continuous hum at harmonics of the power supply frequency. Modern units have been designed with environmental constraints in mind, but big transformers are very expensive devices with a long lifetime so many current substations still involve older units. Such substations were often built at the city periphery, but are now surrounded by residential areas, thus emphasizing noise concern.

When dealing with a potentially noisy site, a significant problem is to be able to characterize the source and separate its noise contribution from other sources. Acoustic measurements may be processed by synchronous demodulation averaged over long enough periods, as any power line fed by the transformer may be used as a phase reference for a lock-in measurement device. This allows to identify the actual contributions from the substation devices, and eventually assess potential emergence of harmonic components from background noise. When a suspect unit is targeted, the next step is to be able to assess if its contribution may be significant at locations around the substation.

As an example, figure 1 shows a medium-sized transformer in a typical substation environment. It is an old 12 MVA, 36/10 kV, 50 Hz unit located near Brussels (Belgium), with coarse size 3m x 3m x 1m. A concrete wall has been built close to the tank, in an attempt to reduce noise at a nearby house. The

Figure 1. Close picture of transformer tank, showing nearby wall, transformer equipments and radiators.

tank cooling requires huge radiators which almost hide it, whereas many small equipments are fitted onto it.

As part of a research project, vibration measurements were performed on this device. They involved a dedicated setup allowing to scan the tank surface with an accelerometer, and to extract its signal synchronously with the power supply. Such a measurement campaign was part of so-called "baseline measurements" dedicated to the design of an active control system. The data collection was a long and painful task tooking around two weeks full time, with many practical difficulties coming from the bad accessibility of the tank surface. The vibration data were then used in a BEM model for the assessment of the transformer contribution to the substation noise and the design of the ANC system. Is was later demonstrated that the field complexity is much higher for the vibration than for the radiated pressure, which complexity decreases rapidly with distance [1, 2]. The high resolution of vibration data is thus only required for the BEM model, which must grasp the vibro-acoustic coupling on the tank.

This led to search a way to compute far-field radiated pressure from data collected as efficently as possible on site. The constraints associated are to be far enough from the tank surface (to reduce both the complexity of the acoustic field and electromagnetic interferences), although staying inside the substation, so coping with the numerous constraints resulting from the surrounding of online high voltage devices. This means that measurement locations are restricted to site-specific ones, preferably involving robust sensors - *i.e.* microphones.

The problem of identifying sound sources has been addressed thoroughly in the litterature, and many approaches have thus been proposed. The most widespreads are the NAH [3, 4, 5, 6] and the matrix-based (BEM+SVD) approach [7, 8, 9, 10]. Reviews of many methods for reconstructing sound sources may be found in references [11, 12, 13].

Because transformer tanks are arbitrarily shaped and surrounded by nearby boundaries, a matrix-based method has been selected. Microphones cannot be very close to the tank, so nearfield techniques cannot be used. Conversely, no back-propagation is needed, as the field has to be computed outside the substation, *i.e.* further away from the measurement locations. This has been addressed by expanding the field over a set of "far-field radiating modes". This approach is briefly described in section 2. Simulations are then presented in section 3, and discussed in section 4.

2. Method

Basically, the approach proposed here is very close to the one initially described in reference [7], and further developed in later papers [9, 10]. It assumes that the shape of the radiating transformer tank and eventual surrounding objects can be described by a surface mesh with sufficient accuracy (at lower frequencies many geometrical details are not relevant and most surfaces may be considered as perfectly reflecting).

Starting from the integral solution for the pressure on the vibrating tank, it is possible to establish a matrix relationship between the volume velocities $\mathbf{q_s}$ of each mesh element and the boundary pressures $\mathbf{p_s}$ on this mesh. This is an impedance matrix which is independant of the actual pressure field, and may be estimated numerically at a given frequency using a BEM code (see §2.1).

This impedance matrix may be expanded over the so-called "radiation modes" (the terminology may differ between references), *i.e.* the basis obtained through a singular values decomposition of the impedance matrix [7, 14, 15]. This builds a set of independant solutions of the radiation problem, each cor-

responding to a pair of "source" (volume velocity) and "receiver" (pressure) vectors on the mesh, associated with a singular value which represents the radiation efficiency of the corresponding solution. By convention, the SVD provides these solution in decreasing order of efficiency; it is thus easy to truncate the set of radiation modes in order to keep only the most efficient ones. This allows to expand a given problem over a limited set of these "radiation modes".

Each "radiation mode" corresponds to a separate radiation problem, for which it is possible to compute the pressure at locations around the transformer tank. Conversely, if a set of pressions is measured at these locations, it is possible to determine the coefficients of the "radiation modes" expansion which is the best approximation of the measured pressure. This is an ill-conditioned inverse problem, which requires a regularization technique (see §2.2). The resulting expansion may then be propagated anywhere outside the transformer tank, thus providing an estimate of the pressure at locations where it was not measured.

2.1. Computation of radiation modes

Denoting Γ the boundary surfaces (tank and eventual objects), the pressure p at location M may be represented by the classical integral formulation :

$$p(\omega, M) = \int_\Gamma [\partial_{\mathbf{n}} G(\omega, M, S) p(\omega, S) - G(\omega, M, S) \partial_{\mathbf{n}} p(\omega, S)] \, d\Gamma(S) \quad (1)$$

assuming a harmonic solution with $e^{+\jmath\omega t}$ time dependance, G denotes the usual Green function $G(R) = e^{-\jmath kR}/4\pi R$ with $k = \omega/c$ (c the sound speed), and $\partial_{\mathbf{n}}$ denotes the normal derivative (outward normal vector). The acoustic velocity $\mathbf{v}$ is related to the pressure by $\nabla p = -\jmath\rho\omega\mathbf{v}$ where ρ is the fluid volumic mass. It is thereafter assumed that the computations are not performed at frequencies close to the singularities of the Dirichlet interior problem.

The exterior problem may be discretized over a suitable (and smooth) mesh so that equation 1 is approximated efficiently assuming piecewise-constant pressures and velocities over the mesh elements. This reduces the continuous integral to a matrix form expressed at the centers of the mesh elements for each value of ω :

$$\frac{1}{2}\mathbf{p_s} = \mathbf{M q_s} - \mathbf{D p_s} \quad (2)$$

The impedance matrix $\mathbf{Z}$ is thus :

$$\mathbf{Z} = p_s q_s^{-1} = [\frac{1}{2}\mathbf{I} + \mathbf{D}]^{-1}\mathbf{M} \quad (3)$$

where $\mathbf{M}$ and $\mathbf{D}$ are computed using an image source if a half space is assumed.

The $\mathbf{Z}$ matrix is classically expanded through a singular value decomposition, however this expansion is dominated by "reactive" components describing the evanescent near-field on Γ. In our case only the real part of $\mathbf{Z}$ is thus expanded, leading to "far-field radiation modes" :

$$\Re(\mathbf{Z}) = \mathbf{U\Sigma V}^\dagger \quad (4)$$

where † denotes the matrix transconjugate. Each column of $\mathbf{V}$ is a real vector of volume velocities on the mesh, while the corresponding column of $\mathbf{U}$ is a complex vector of pressures at the element centers. The $\mathbf{\Sigma}$ matrix is diagonal and contains positive real values (radiation efficiencies). Columns of $\mathbf{V}$ and $\mathbf{U}$ may be used in a discretized version of equation 1 to obtain the matrix $\mathbf{H}$ of transfer functions between modes (now considered as "equivalent sources") and locations anywhere outside Γ.

2.2. Identification of equivalent source

The number N_{sv} of "radiation modes" to consider may be determined from the radiation efficiencies provided by matrix $\mathbf{\Sigma}$. These efficiencies are conveniently plotted as a cumulative weight, in a way similar to figure 3. This allows to select a number of modes from a target accuracy.

The number of microphones should then be somewhat superior to the selected number of modes, in order to build an overdetermined system. Microphones locations cannot be chosen arbitrarily because of the many constraints in an actual substation. Starting from a set of "possible locations", a selection is made by ensuring roughly that each "radiation mode" is close to its maximum for at least one location (several if possible for the most efficient terms). No further optimization has been considered in this work as this would hardly be achievable on site.

Mode coefficients $\mathbf{d}$ are then obtained from the measured pressures $\mathbf{p_m}$ through a matrix pseudo-inverse. As this is an ill-conditioned problem, two regularization methods have been compared for the determination of $\mathbf{d}$, following the relation below :

$$\mathbf{d} = [(\mathbf{H_m^*}\,\mathbf{H_m}) + \mu\mathbf{I}]^+_{(N_k)} \mathbf{H_m^*}\,\mathbf{p_m} \quad (5)$$

where $\mathbf{H_m}$ is the submatrix of $\mathbf{H}$ at the measurement locations, $[.]^+_{(N_k)}$ denotes a pseudo-inversion by SVD truncated to N_k singular values, and μ is a penalization coefficient (variant of Tikhonov regularization). When keeping all radiation modes ($N_k = N_{sv}$), regularization may be tuned by the value of μ. Conversely, this value may be reduced to a marginal or null value, and regularization tuned by selecting $N_k < N_{sv}$. The combination was not tested.

The far-field can then be computed as a superposition of the radiation modes, by multiplying the relevant part of $\mathbf{H}$ by the $\mathbf{d}$ coefficients.

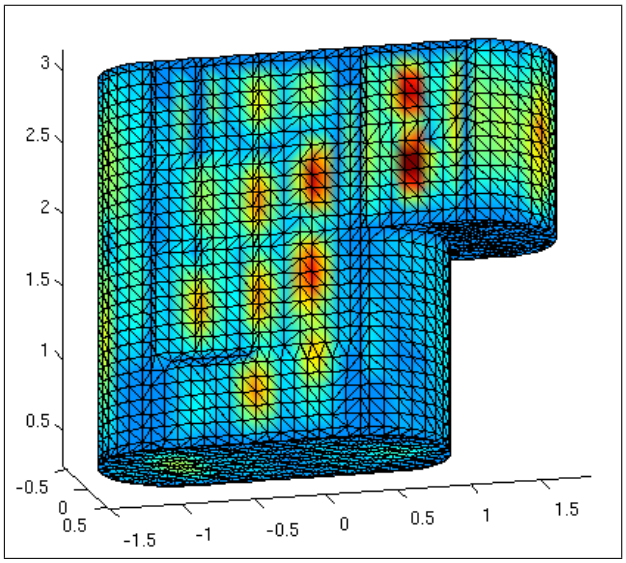

Figure 2. Mesh of transformer tank, showing acceleration measured at 100 Hz.

3. Simulations

Figure 2 shows the mesh geometry corresponding to the transformer pictured in figure 1. It comprises 5676 triangular elements formed from 2840 nodes. The tank is located about 0.35m above a reflecting plane at $z = 0$, but no other reflecting object is considered here. The acceleration measured at 100 Hz during the baseline measurements is also represented. This measured acceleration is the input of an indirect BEM computation using the Sysnoise © software, leading to simulations of the required "measured pressures" (*i.e.* target field).

The radiation modes are computed using a dedicated BEM code ("FELIN", developped at LMA) following a method similar to the one exposed in §2.1. The corresponding cumulative weights are presented by figure 3 for two frequencies of interest : 100 Hz (blue) and 200 Hz (red). This shows that most of the tank radiation may be computed using less than 30 radiation modes at 100 Hz and less than 70 radiation modes at 200 Hz. This is significantly lower than the number of mesh elements.

Pressures are computed for the target field and each of the radiation modes at many locations around the transformer : seven cylinders of radii in geometric progression from 3m to 24m, each comprising 72 angular positions at 11 heights regularly spaced between 0 and 5m. This results in 5544 locations (792 for each radius) ranging from "almost-near" to "far" from the tank. No higher location has been considered, as this would certainly not be allowed in an actual substation. The "measurements" locations were selected among the first cylinder, *i.e.* at a distance from the tank of the same order of magnitude as its size (which seems realistic for usual sites).

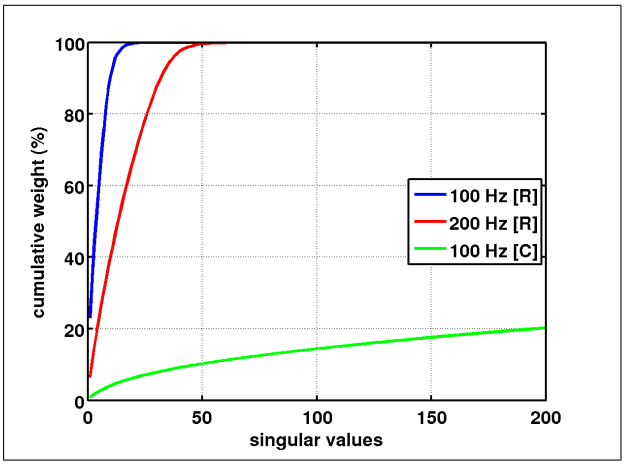

Figure 3. Cumulative weight of singular values computed at 100 and 200 Hz

A mean error E has been computed from the target pressures P_t and reconstructed pressures P_r for points of the last cylinder, assumed to be in far-field. E is the RMS error over all these locations, normalized by the average RMS pressure ($E^2 = \sum(||Pr - Pt||^2)/\sum(||Pt||^2)$), expressed in dB. A pressure map over the reflecting plane has been drawn as an illustration of the spatial repartition of the target field at various distances, and its reconstruction.

The penalization coefficient μ or the number N_k of SVD terms kept during the pseudo-inversion has been chosen following the classical "L-curve" method. Comparison of these two regularization means showed a "better performance" of SVD truncation, which seems to require less "measurements" for a given error in far-field.

3.1. Identification at 100 Hz

Considering the first harmonic of transformer noise, at 100 Hz, the tank dimensions are close to the acoustic wavelength. Identification of the target field from the "measurements" required 26 "radiation modes", leading to a RMS pressure error in far-field of about -13dB. The corresponding maps are presented by figure 4 : the targer field is illustrated by the top map, and its reconstruction by the middle one.

Such a graphical comparison has a limited value, but it illustrates that the general shape of the wavefront is adequately reproduced at all ranges between the "measurement" radius and the far-field. This simulation is obtained using 32 "measurements", *i.e.* about 25% more than the number of radiation modes.

3.2. Identification at 200 Hz

For the second harmonic (at 200 Hz), the tank dimensions are about two times larger than the wavelength. Identification of the target field from the "measurements" required 47 "radiation modes", leading to a

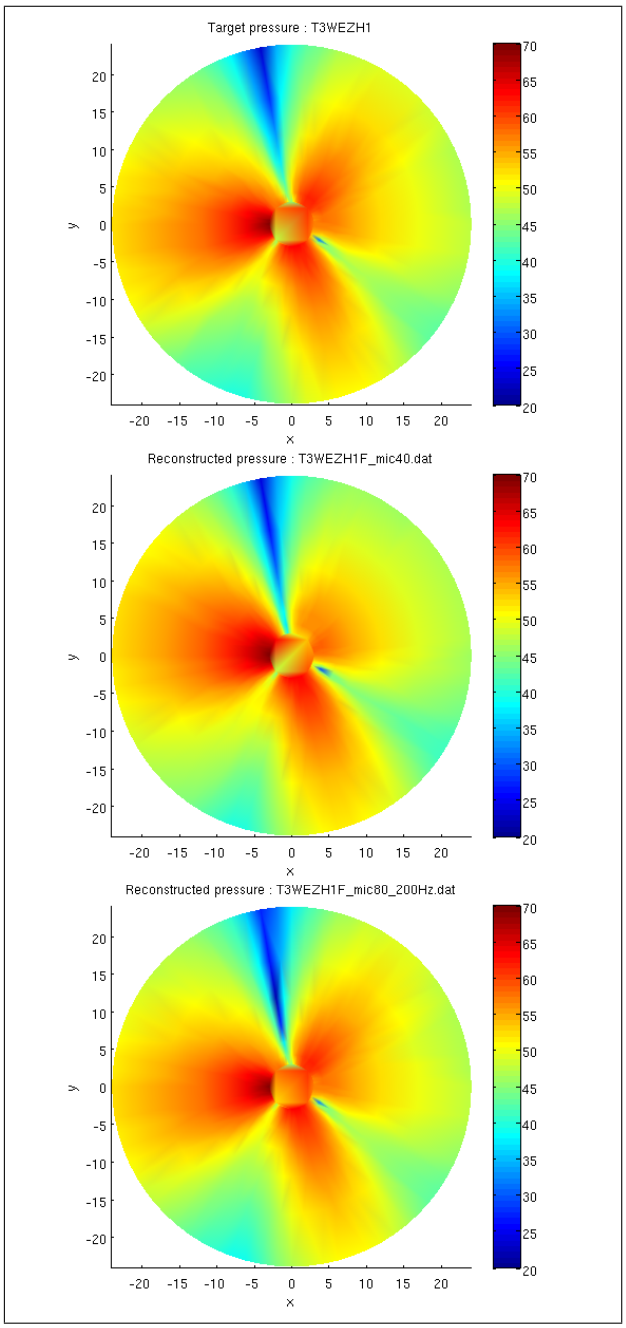

Figure 4. Pressure maps at 100 Hz : target (top), reconstructed using 26 SV100 (middle), reconstructed using 51 SV200 (bottom). x and y in m; color scale in dB

RMS pressure error in far-field of about -9dB. The corresponding maps are presented by figure 5.

Again the general shape of the wavefront is adequately reproduced at all ranges between the "measurement" radius and the far-field. This simulation is obtained using 64 "measurements", *i.e.* about 35% more than the number of radiation modes.

It should be noted that the "measurement" locations may differ between 100 Hz and 200 Hz, as the corresponding "radiation modes" are different. From a practical point of view, it would be possible to keep the same locations, which have not been especially

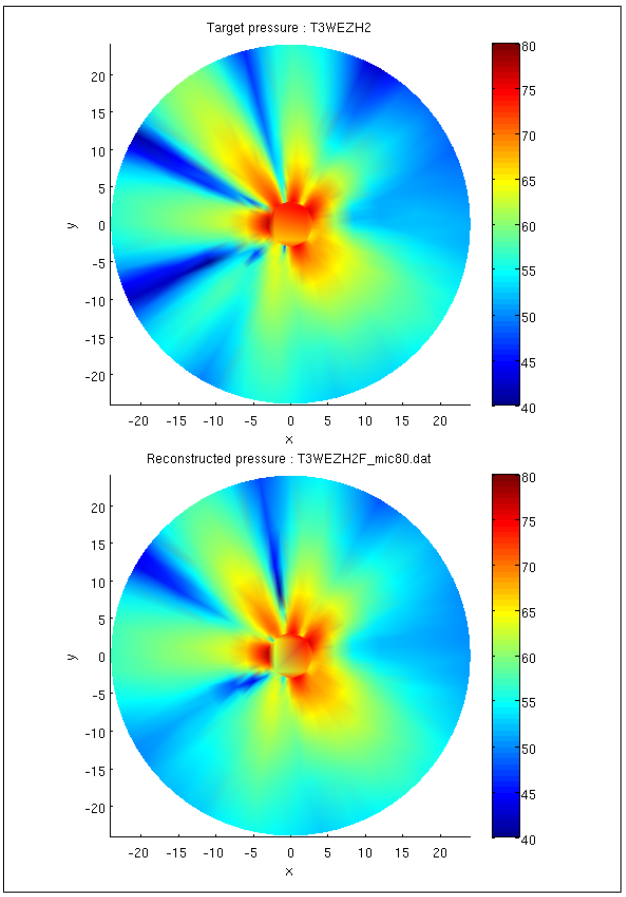

Figure 5. Pressure maps at 200 Hz : target (top), reconstructed using 47 SV200 (bottom). x and y in m; color scale in dB

optimized here. This would of course lead to a better approximation at 100 Hz : by using 64 measurement locations instead of 32, more coefficients of the 100 Hz radiation modes (labelled SV100) can be identified.

The above simulations consider each frequency as a separate problem. Indeed the "radiation modes" are frequency-dependant, as they involve the wavenumber in the BEM model. Reference [16] however states that "the radiating subspace at a certain frequency f_1 is a subspace of the radiating subspace at frequency $f_2 > f_1$". This would imply that the "radiation modes" computed for 200 Hz (labelled SV200) could be used to expand the field radiated at 100 Hz. This has been checked, and a quite good reconstruction could be obtained at 100 Hz keeping 51 of the SV200 modes, leading to a far-field RMS error around -24dB. It is illustrated by figure 4 (bottom map).

4. Discussion

The work presented in this paper is based on well-known methods for reconstructing a source radiation. It is adapted to the case of transformer monitoring by expanding only the real part of the radi-

ation impedance, thus requiring a reasonable number of pressure measurements. Green curve of figure 3 shows the cumulative weight of singular values for the complex **Z** matrix; the number of terms required to reconstruct the total pressure on the tank would be huge, which shows the importance of removing the imaginary part of **Z** when reconstructing the far field from a limited number of measurements.

The major advantage of this approach is that it uses the a-priori knowledge of the radiation modes of the vibrating object, obtained numerically from a BEM model based on a coarse description of the tank geometry. This is also a potential drawback, as any weakness of this model may impact significantly the accuracy of the reconstructed pressure. The geometry of all boundaries must therefore be recorded carefully on site, a task which requires acoustic skills to grasp all relevant informations. Computation of the radiation modes are performed using a custom BEM code, taking about 20 minutes on a recent computer. It seems that the resulting series may be used for a frequency band at least equal to an octave, so the numerical cost seems quite reasonable nowadays.

For measurements close to the vibrating surface, the strong reactive near-field pressure may bias the identification, which only considers far-field radiation modes. This does not seem to be problematic when measurements are performed at a distance of the same ordre of magnitude than the tank, as simulated here. Additional reactive radiation modes could be included in the expansion if needed.

The number and location of pressure measurements is a major concern, together with the determination of optimal regularization parameters - both aspects are tightly linked. Here, the number of efficient "radiation modes" is estimated from the BEM model, and a number of measurements about 50% greater seems to be conservative, measurement locations seeming thus not critical. The determination of the expansion coefficients using a regularization by truncated SVD appeared as relevant, as it may be tuned from the signal-to-noise ratio of the measurements (quite good with synchronous demodulation over long integration time). Alternative sensing strategies are described in recent papers [17, 18, 19] and might be considered for further work.

Acknowledgement

The authors would like to thank the company that gave us access to their transformer, and especially to Jos Staas for his help and support during the measurements. These were performed while the first author was employee of Ecole Polytechnique Fédérale de Lausanne (EPFL), Switzerland.

References

[1] O. Schevin, "Contribution à l'étude des modes de rayonnement acoustique d'une structure", *PhD Thesis EPFL*, Lausanne (2001).

[2] Ph. Herzog and O. Schevin, "Estimation du degré de complexité d'un modèle de source vibrante", *Proc. 6th French Congress on Acoustic (CFA)*, Lille, France (2002).

[3] E.G. Williams, J.D. Maynard, E. Skudrzyk, "Sound source reconstructions using a microphone array", *J. Acoust. Soc. Am.* **68(1)**:340-344 (1980).

[4] E. G. Williams, "Fourier Acoustics: Sound Radiation and Nearfield Acoustical Holography", *Academic Press*, London (1999).

[5] A. Sarkissian, "Extension of measurement surface in near-field acoustic holography", *J. Acoust. Soc. Am.* **115(4)**:1593-1596 (2004).

[6] C. Langrenne, M. Melon, A. Garcia, "Boundary element method for the acoustic characterization of a machine in bounded noisy environment", *J. Acoust. Soc. Am.* **121(5)**:2750-2757 (2007).

[7] W.A. Veronesi, J.D. Maynard, "Digital holographhic reconstruction of sources with arbitrarily shaped surfaces", *J. Acoust. Soc. Am.* **85(2)**:588-596 (1989).

[8] G.V. Borgiotti, "The determination of the far field of an acoustic radiator from sparse measurement samples in the near field", *J. Acoust. Soc. Am.* **92(2)**:807-818 (1992).

[9] M.R. Bai, "Application of BEM (boundary element method)-based acoustic holography to radiation analysis of sound sources with arbitrarily shaped geometries", *J. Acoust. Soc. Am.* **92(1)**:533-549 (1992).

[10] B-K Kim, J-G Ih, "On the reconstruction of the vibro-acoustic field over the surface enclosing an interior space using the boundary element method", *J. Acoust. Soc. Am.* **100(5)**: 3003-3016 (1996).

[11] E.G. Williams, "Comparison of SVD and DFT approaches for NAH", *Proc. InterNoise*, Dearborn (2002).

[12] M.B.S. Magalhães, R.A. Tenenbaum, "Sound sources reconstruction techniques : a review of their evolution and new trends", *Acta Ac. u Ac.* **90**:199-220 (2004).

[13] S.F. Wu, "Methods for reconstructing acoustic quantities based on acoustic pressure measurements", *J. Acoust. Soc. Am.* **124(5)**:2680-2697 (2008).

[14] G. V. Borgiotti, "The power radiated by a vibrating body in an acoustic fluid and its determination from boundary measurements", *J. Acoust. Soc. Am.* **88(1)**:1883-1893 (1990).

[15] A. Sarkissian, "Acoustic radiation from finite structures", *J. Acoust. Soc. Am.* **90(1)**:574-578 (1991).

[16] G. V. Borgiotti and K. E. Jones, "Frequency independence property of radiation spatial filters", *J. Acoust. Soc. Am.* **96(6)**: 3516-3524 (1994).

[17] Q. Leclère, "Acoustic imaging using underdetermined inverse approaches : frequency limitations and optimal regularization", *J. Sound Vib.* **321**:605-619 (2009).

[18] J. Antoni, "A Bayesian approach to sound source reconstruction : optimal basis, regularization, and focusing", *J. Acoust. Soc. Am.* **131(4)**:2873-2890 (2012).

[19] G. Chardon, L. Daudet, "Near-field acoustic holography using sparse regularization and compressive sampling principles", *J. Acoust. Soc. Am.* **132(3)**:1521-1534 (2012).